

Chapter 7

Weathered Biotite: A Key Material of Radioactive Contamination in Fukushima



Toshihiro Kogure, Hiroki Mukai, and Ryosuke Kikuchi

Abstract The eastern area of Fukushima Prefecture, where the Fukushima Daiichi nuclear power plant is located, is covered mainly with weathered granitic soil originated from the geology of this area. Weathered biotite (WB), or partially to almost vermiculitized biotite, is abundant in the soil. WB has frequently been found as radioactive soil particles sorbing radiocesium and has been identified as “bright spots” by autoradiography. Laboratory experiments using the ^{137}Cs radioisotope indicated that WB collected from Fukushima sorbed ^{137}Cs far more efficiently than other clay minerals from ^{137}Cs solutions whose concentration was comparable to that expected for the radioactive contamination in Fukushima. This supports the abundance of radioactive WB particles in the actual contaminated soil. The Cs-desorption property of WB was also different from those of other minerals. If the period of immersion in the Cs solution was more than a few weeks, the sorbed Cs in the WB were hardly desorbed by ion-exchange with any electrolyte solutions. These results imply that decontamination of the radioactive soils is difficult if using “mild” chemical treatments and that most radioactive Cs are now fixed stably (dare one say “safely”) by WB in the soil of the Fukushima area.

Keywords Weathered biotite · Radioactivity · Cesium · Sorption · Contaminated soil · Desorption · Frayed edge sites · Ion-exchange

7.1 Introduction

The accident at the Fukushima Daiichi nuclear power plant (FDNPP) in March 2011 released a significant amount of radiocesium (Cs), which caused serious and long-term radioactive contamination of the land around the power plant. It is essential to understand the state and dynamics of radiocesium in the environment to consider its

T. Kogure (✉) · H. Mukai · R. Kikuchi

Department of Earth and Planetary Science, Graduate School of Science, The University of Tokyo, Tokyo, Japan

e-mail: kogure@eps.s.u-tokyo.ac.jp; h-mukai@aist.go.jp; rkikuchi@eps.s.u-tokyo.ac.jp

© The Author(s) 2019

T. M. Nakanishi et al. (eds.), *Agricultural Implications of the Fukushima Nuclear Accident (III)*, https://doi.org/10.1007/978-981-13-3218-0_7

influence on life, agriculture, the decontamination processes, etc. in Fukushima at present and in the future. More than 6 years after the accident, our knowledge of radiation and radiocesium in Fukushima has been increased owing to the work of a number of research groups in Japan. For instance, measurements of the depth profile of radiation in the soil revealed that most radiocesium remains at a shallow depth and it hardly moves downward with time (e.g., Honda et al. 2015), which suggests that radiocesium is being trapped rigidly in specific materials such as clay minerals in the soil. Many researchers have suggested, mainly based on laboratory experiments, that micaceous minerals such as illite and vermiculite are important for the sorption and retention of Cs in the soil (Comans et al. 1991; Cornell 1993; Evans et al. 1983; Francis and Brinkley 1976; Poinssot et al. 1999; Zachara et al. 2002). For instance, Cornell (1993) summarized the potential adsorption sites for Cs in the micaceous minerals as follows: (1) cation exchange sites on the surface, (2) layer edge sites, (3) frayed edge sites (FES), and (4) internal interlayer sites. Among them, it has been suggested that FES, which are formed around the edges of platy micaceous crystals by weathering, strongly and selectively adsorb Cs (Brouwer et al. 1983; McKinley et al. 2004; Nakao et al. 2008). However, it was not certain whether such micaceous minerals really retain radiocesium in the soil around Fukushima. By analyzing the contaminated soils in Fukushima, we first reported that WB or partially vermiculitized biotite, originating from granitic rocks which constitute the geology of this area, is a dominant sorbent of radiocesium (Mukai et al. 2014). Next, we demonstrated by laboratory experiments that WB sorbed Cs more efficiently than other clay minerals from solutions if the Cs concentration in the mineral was dilute, as in the actual soil in Fukushima (Mukai et al. 2016a).

This paper reviews our recent research with respect to WB in Fukushima, including its structure and Cs-sorption/desorption properties, and discusses the role of WB in the radioactive contamination in Fukushima. Details of the experiments to obtain the results presented here are described in the original papers already published (Mukai et al. 2014, 2016a, b; Kikuchi et al. 2015; Motai et al. 2016).

7.2 Speciation of the Radioactive Particles in the Soil of Fukushima

Although the air dose rate in the areas around FDNPP is quite high due to radiocesium in the soil, the actual concentration of radiocesium in the soil is generally too low to specify its location, even if using recent advanced micro-analytical techniques such as X-ray microanalysis with synchrotron radiation. At present, only autoradiography, which is capable of detecting radiation with a certain (but not enough) spatial resolution, is a practical method for finding radioactive particles in the soil. Autoradiography using imaging plates (IPs), which are reusable and detect radioactive rays efficiently and proportionally to the intensity of radiation, has been applied frequently to find the distribution of radiation or radiocesium in various

samples including soils, plant tissues, feathers of birds, etc. (e.g., Nakanishi 2016). IP autoradiography of the samples from Fukushima often showed an inhomogeneous distribution of radiation in the samples, represented by a number of “bright spots” in the IP images obtained by placing the IPs in contact with the samples for a certain time. However, results or reports that identified the materials forming the bright spots were few.

Mukai et al. (2014) collected soil particles of around 50 μm in size by sieving litter soil collected from Iitate village. The soil radioactivity was $\sim 10^6$ Bq/Kg, and the researchers dispersed the soil particles directly on a special IP which had a fine grid pattern formed by a laser marker (Fig. 7.1a). Using the grid pattern, the soil particles which formed bright spots were easily located under an optical microscope (Fig. 7.1b–d). Then the radioactive particles were picked up by a vacuum tweezer on a micro-manipulator (Fig. 7.2), and moved onto a substrate with double-stick tape for electron microscopy. About 50 radioactive particles were characterized by their morphologies and chemical compositions by a scanning electron microscope (SEM) with an energy-dispersive X-ray spectrometer (EDS), and they were roughly divided into three types: an aggregate of fine mineral particulates, particles rich in organic matter, and “weathered biotite” (Fig. 7.3) (Mukai et al. 2014). The particle

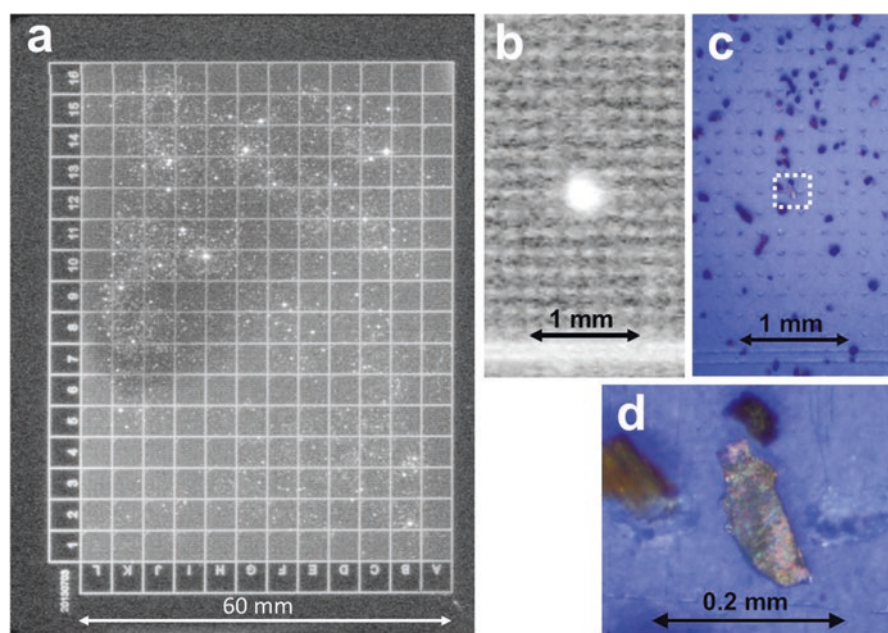


Fig. 7.1 (a) Readout image from an imaging plate (IP, Fuji Film FDL-UR-V) with a grid pattern formed using a laser marker, and with radioactive soil particles dispersed on the IP and exposed for around 1 week in a dark box. (b) Magnified readout image including a “bright spot” with the image of the grid pattern. (c) The position of the IP corresponding to the image in (b). (d) The soil particle corresponding to the bright spot in (b). Probably the particle is weathered biotite, considering its platy morphology. (Mukai et al. 2014)

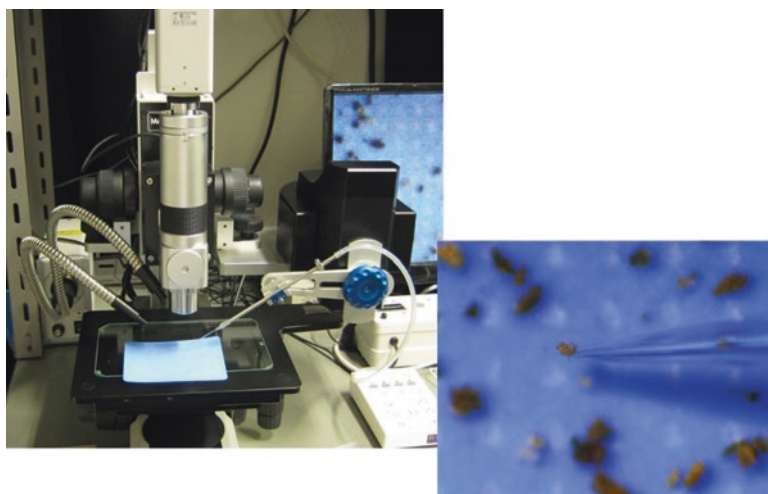


Fig. 7.2 (Left) High-magnification stereomicroscope with a micro-manipulator, used to pick up the soil particles dispersed on IPs. Vacuum tweezers (an evacuated capillary tube) are attached to the micro-manipulator. (Right) A soil particle picked up by the capillary tube

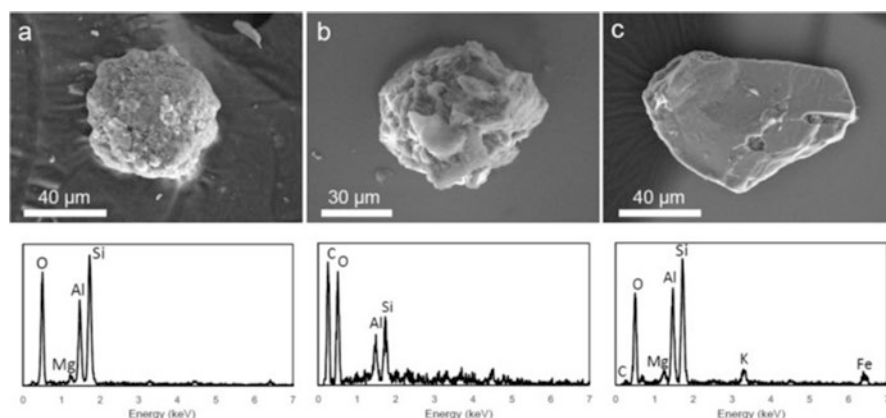


Fig. 7.3 SEM images (upper) and EDS spectra (lower) from the whole particle for typical radioactive soil particles found by IP autoradiography. (a) Aggregate of fine mineral particulates. (b) Particle consisting of organic matter and a small amount of minerals. (c) Weathered biotite with a platy shape. (Mukai et al. 2014)

shown in Fig. 7.3b had a definite platy morphology indicating a mono-crystalline phyllosilicate mineral and had a composition similar to biotite but with less potassium than normal biotite. It is well known that biotite partially changes gradually into vermiculite by the oxidation of iron and by losing potassium through weathering. Here we call such partially vermiculitized biotite “weathered biotite (WB)”. The population ratios of the three types of radioactive particles were almost the

same. The radioactivity of each particle estimated from the intensity of the IP signal was in the range of 0.005 ~ 0.05 Bq (Motai et al. 2016), which is far lower than that (a few Bq per particle) of radiocesium-bearing microparticles emitted directly from the broken pressure vessel of FDNPP (Adachi et al. 2013; Yamaguchi et al. 2016).

7.3 Mineralogical Characterization of Weathered Biotite (WB)

The western side of FDNPP is a mountainous area named the Abukuma highland, which consists of granitic rock (Abukuma granitic-body). This granitic rock has been altered by weathering during a geological time to a thick sandy soil called “Masado” in Japanese (Fig. 7.4). By erosion and sedimentation, Masado is spread over forests, agricultural fields, and residential areas in this region. WB is abundant in Masado because biotite is a major constituent mineral of granite. Biotite is structurally classified into a trioctahedral 2:1 type phyllosilicate, and its composition can be roughly expressed as $K(\text{Mg}, \text{Fe}^{2+}, \text{Fe}^{3+})_3\text{Si}_3\text{AlO}_{10}(\text{OH}, \text{F})_2$. Due to weathering on the terrestrial surface, ferrous irons in biotite were oxidized to ferric, which resulted in the leaching of potassium (K) ions and substitution by hydrated magnesium or calcium ions at the interlayer site between the silicate layers. Due to the substitution or hydration, the interlayer space is expanded by ca. 0.4 nm, increasing the thickness of the unit layer from 1.0 nm to 1.4 nm. If this substitution is complete, the resultant



Fig. 7.4 Weathered granitic soils or “Masado” consisting of hills in Fukushima (Ono-Town, Tamura-county, Fukushima Prefecture). The rounded rocks are original granite buried in the soil

new mineral is called “vermiculite”. However, WB is generally at an intermediate stage between biotite and vermiculite, forming interstratification of the K-occupied (biotite) and hydrated (vermiculite) interlayers. Such an interstratified structure can be identified directly using recent high-resolution transmission electron microscopy (HRTEM). Figure 7.5 shows a HRTEM image of biotite-vermiculite interstratification in WB collected from Fukushima. The arrowed interlayer regions where the contrast of K is missing were originally occupied by hydrated Ca^{2+} or Mg^{2+} forming a larger space but collapsed due to dehydration in the vacuum in TEM (Kogure et al. 2012). X-ray diffraction (XRD) of WB in Fukushima shows various complicated patterns, depending on the ratio of biotite and vermiculite interlayers, and their mixing feature (Fig. 7.6) (Kikuchi et al. 2015). If WB is immersed in a concentrated Cs solution experimentally, Cs selectively substitutes the hydrated interlayer sites, as revealed by the distinct bright contrast of Cs in the high-angle-annular-dark-field (HAADF) scanning TEM (STEM) image (Fig. 7.7) (Okumura et al. 2014; Kikuchi et al. 2015). However, considering its radioactivity (~ 0.1 Bq per particle), the actual concentration of radiocesium in the radioactive WB in Fukushima is extremely low compared to the concentration of the artificially Cs-sorbed WB like that shown in

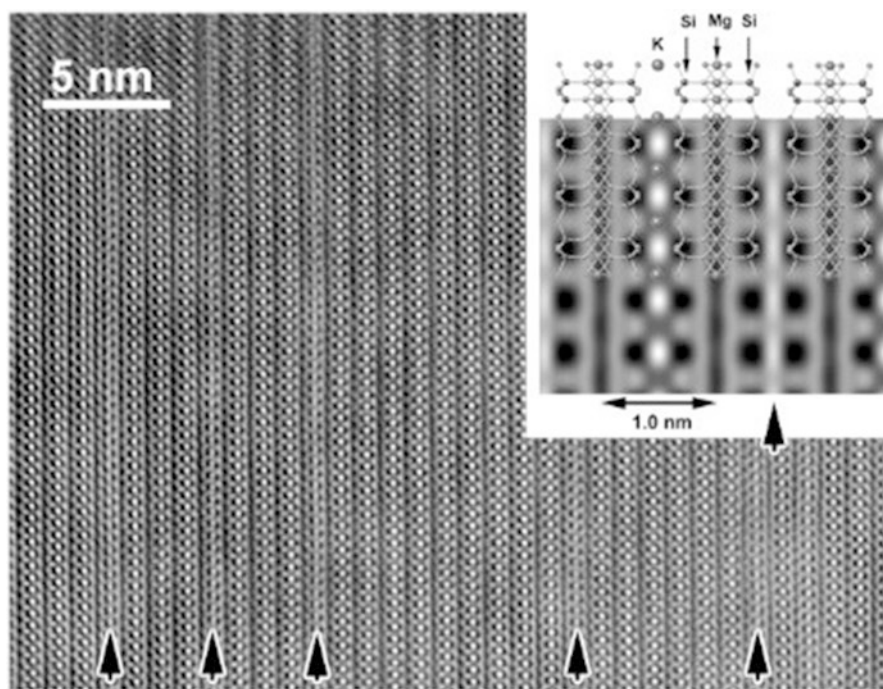


Fig. 7.5 High-resolution transmission electron microscope (HRTEM) image of biotite-vermiculite interstratification in the weathered biotite collected from Fukushima. The arrowed interlayer regions where the contrast of potassium is missing were originally hydrated but collapsed by dehydration in the vacuum in TEM. The inset at the top-right is the simulated contrast for the biotite structure with the potassium (K)-occupied (left) and K-missing (right) interlayers

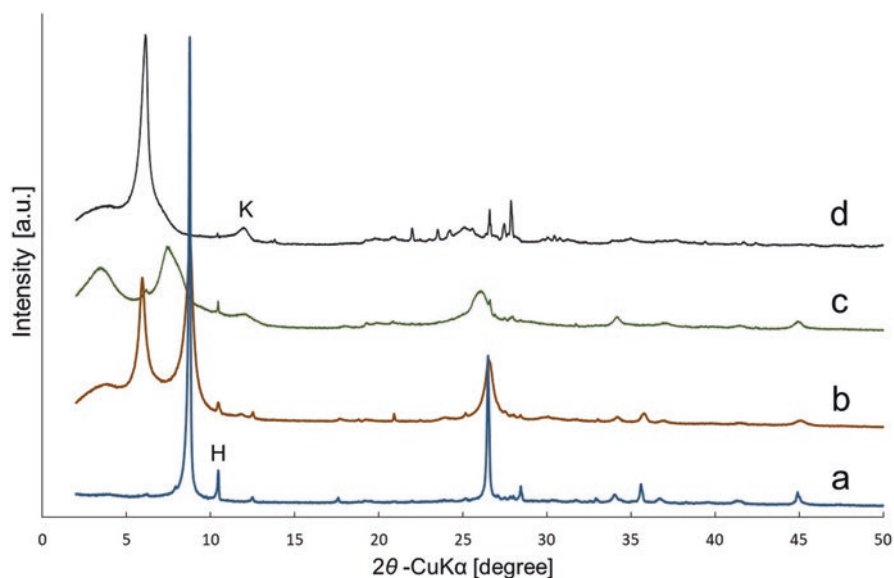


Fig. 7.6 Oriented XRD patterns of various “weathered biotite” specimens in Fukushima. (a) Almost fresh or original biotite taken from granite. (b) Interstratification of the biotite and vermiculite layers. The biotite layers are dominant and the two types of layers are rather segregated. (c) Finely-mixed interstratification of the biotite and vermiculite layers. (d) Interstratification of the two types of layers and the vermiculite layers are dominant. The broad peak marked with “K” is kaolinite or halloysite, and the sharp peak marked with “H” is hornblende. (Kikuchi et al. 2015)

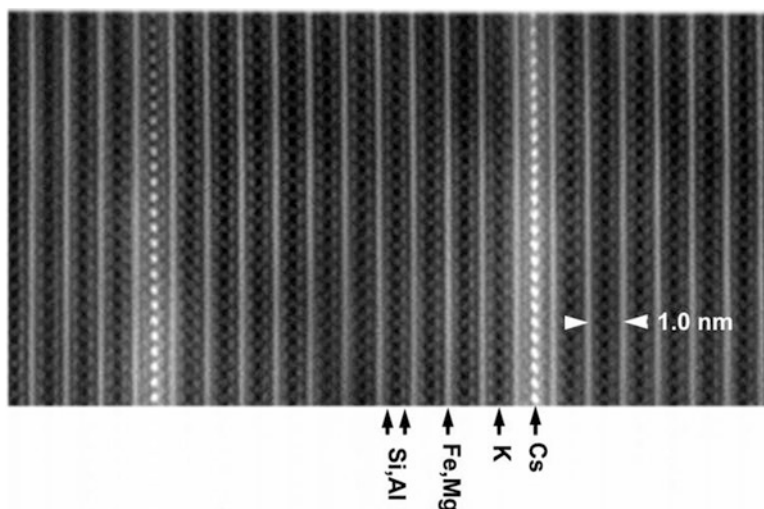


Fig. 7.7 High-angle annular dark-field (HAADF) image of weathered biotite to which cesium was sorbed experimentally, recorded using a scanning transmission electron microscope (STEM). (Kikuchi et al. 2015)

Fig. 7.7. Hence, direct localization of radiocesium sorbed in the weathered biotite by high-resolution electron microscopy or any micro-analytical techniques is not possible. We need to apply other techniques to determine (or at least form a conjecture on) the sorption site for the radiocesium in WB.

As stated above, several researchers have demonstrated experimentally that micaceous minerals such as illite and vermiculite have a high affinity with Cs, and have suggested that this property is due to the FES located around the edge of the platy crystals of the minerals, where Cs with a larger ionic radius than other alkali ions are thought to be selectively and strongly fixed owing to the tapered interlayer spaces (Mckinley et al. 2004; Poinssot et al. 1999; Zaunbrecher et al. 2015). To consider its correctness and the actual sorption sites of radiocesium in WB, the following experiment was conducted (Mukai et al. 2016b). In general, the special resolution of IP autoradiography is not good enough to distinguish the distribution of radiation in a radioactive particle of even a few hundred microns. Instead, we cut platy radioactive WB crystals using a focused-ion-beam (FIB) micro-processing instrument into several fragments and separated them from each other enough that they could be resolved in the IP autoradiography using the micro-manipulator (Fig. 7.2). As shown in Fig. 7.8, all the fragments had similar radiation, regardless of the location in the grain, or with/without the original edge of the platy crystal, indicating that radioactivity was not concentrated around the edge but rather homogeneously distributed in the crystal. However, it is unlikely that radiocesium is diffused deeply inside the crystal structure of WB in Fukushima. The actual particles of WB are not uniformly dense but have a laminated structure with many open spaces caused by cleavages of biotite (Fig. 7.9). Probably, solutions containing radiocesium easily filled the spaces by capillary action and Cs was sorbed to appropriate sites on the cleaved surfaces of WB. This issue will be discussed further in the next section.

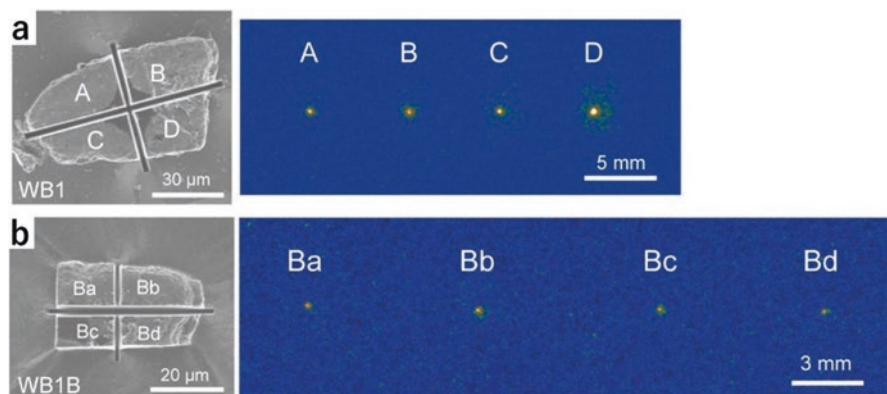


Fig. 7.8 (a) SEM image of radioactive WB cut into four fragments by FIB, and a readout IP image from the four fragments, after separating them from each other. (b) SEM image of the fragment “B”, cut into four fragments, and readout IP image of the four fragments, after separating them from each other. (Mukai et al. 2016b)

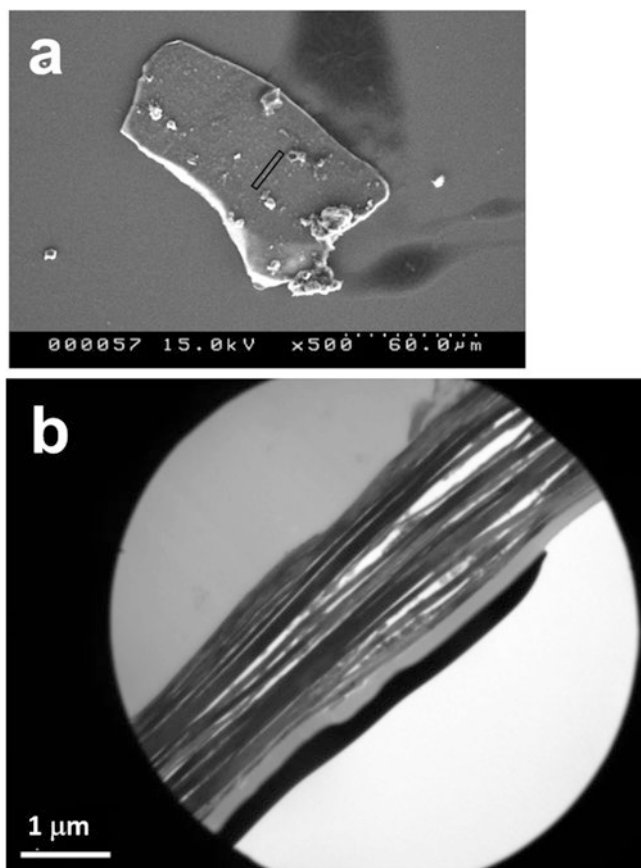


Fig. 7.9 (a) SEM image of a radioactive WB from which the cross-sectional thin section for TEM was fabricated by FIB, from the area indicated with the elongated square around the center. (b) Cross-sectional TEM image of the WB in (a), showing a laminated structure with many cleavages and spaces. (Mukai et al. 2014)

7.3.1 Sorption and Desorption Behavior of Cs to WB

Based on the analyses of the radioactive soil particles in the field as described above, it is suggested that WB is an important material sorbing radiocesium in the soil, influencing the dynamics and fate of radiation in the soil around Fukushima. Hence, we investigated the Cs-sorption/desorption properties of this mineral in the laboratory. For instance, a question to be answered is why WB was frequently found as radioactive soil particles in Fukushima? Was it owing to the abundance of WB in Fukushima or its superior Cs-sorption ability? A study by NIMS (the URL is provided in the Reference section) which surveyed the Cs-sorption ability of various clay minerals after the accident indicated that WB (vermiculite in the study) does not predominantly sorb Cs, in contrast to other micaceous clay minerals like illite and smectite.

However, these data were obtained using a solution with a cesium concentration as low as sub-ppm ($\sim 10^{-5}$ mol L⁻¹). It is natural to expect that the Cs-sorption ability of minerals is dependent on the concentration of cesium in the solution and/or the solid-solution ratio because there are various sorption sites in the minerals. The actual concentration of radiocesium in the rain which caused the radioactive contamination of the soil in Fukushima is considered to be very low. For instance, the amount of rainfall in Iitate village, a seriously contaminated area in Fukushima, over a few weeks after the nuclear accident was around 10 mm according to the records of the Japan Meteorological Agency (the URL is provided in the Reference section). On the other hand, the amount of ¹³⁷Cs per unit area deposited on Iitate village was $\sim 10^6$ Bq/m², according to a report by JAEA (the URL is provided in the Reference section). From these values, the concentration of radiocesium in the rain should have been of the order of 10 ppt (10^{-10} mol L⁻¹). To discuss the contamination event affecting the Fukushima soil, sorption experiments should be conducted with such a low concentration. However, this is close to or below the detection limit of the most sensitive analytical instruments. This problem is solved if radiocesium itself is used as the cesium source and the sorption/desorption amount is estimated by measuring the radiation of the sorbed radioisotope, as used in previous studies (Poinssot et al. 1999; Ohnuki and Kozai 2013). Moreover, we evaluated the sorption amounts of ¹³⁷Cs in the minerals by measuring the radiation in the individual mineral particles quantitatively using IP autoradiography, instead of counting gamma-rays. An advantage of using IP autoradiography is that we can investigate a reaction between a solution and *multi*-minerals. Such reaction can reproduce more practically the event in which radiocesium in the rain was sorbed to the soil composed of several mineral species.

The following RI experiment was conducted: Several mineral species including WB, with four or five particles ~ 50 μ m in size for each species, were arranged within an area of ~ 6 mm \times 6 mm on an acrylic substrate with double-stick tape. Then, 50 μ L solutions containing 3.7, 37 and 370 Bq/mL (0.185, 1.85 and 18.5 Bq in the solutions) of ¹³⁷Cs were dropped to cover all the particles on the substrates. After immersion in the solutions for a certain time, the substrates were washed away with running water and dried, then placed in contact with an IP. The readout images of the IPs are presented in Fig. 7.10. Under all conditions with different ¹³⁷Cs concentrations and immersion periods, the amount of ¹³⁷Cs sorbed by WB collected from Fukushima was much higher than that by other minerals. In the case of lower concentrations of ¹³⁷Cs and/or shorter reaction periods, radiation was detected only from WB. At the concentration of 18.5 Bq/50 μ L and with a reaction length of 1 day, the amount of ¹³⁷Cs sorbed by WB was about two orders of magnitude higher than that sorbed by the other clay minerals. These results definitely indicate that WB has an ability to sorb radiocesium very efficiently in the soil of Fukushima, and our observation above, that WB was frequently found as the radioactive soil particles in Fukushima, is reasonable. Besides its high Cs-sorption ability, the Cs-sorption mechanism of WB at a low concentration is probably different from that of other minerals such as smectite. Figure 7.11 shows the amount of radiocesium sorbed to WB and ferruginous smectite (SWa-1, a reference sample of Clay Mineral Society, USA) as a function of immersion time in the Cs solution. For smectite, the sorption

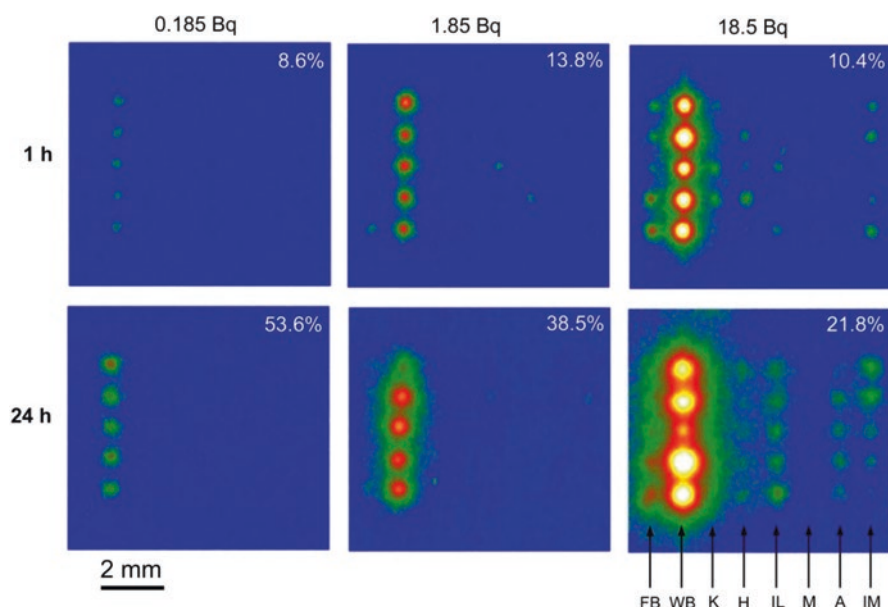


Fig. 7.10 A matrix of the readout images of IPs exposed by the substrates with various mineral particles (five particles for each species) sorbed radiocesium from the solutions. The radioactivity input to the solution and reaction time are at the top and left, respectively. The figure at the top-right of each image is the percentage of radioactivity (or ^{137}Cs) sorbed to the whole mineral particles, estimated from the IP signal. The abbreviations at the bottom-right mean FB: fresh biotite, WB: weathered biotite, K: kaolinite, H: halloysite, IL: illite, M: montmorillonite, A: allophan, IM: imogolite. (Mukai et al. 2016a)

was completed very quickly (probably in less than 1 h) but for biotite, the progress of the sorption was slow, continuing probably more than 1 day.

Next, we investigated the Cs-desorption property of WB, using the Cs-sorbed WB particles prepared by the experiments in Fig. 7.10. In the experiments, substrates with the ^{137}Cs -sorbed WB particles were immersed in various electrolyte solutions and the amount of leached radioactive Cs was estimated also by IP autoradiography before and after the immersion (Fig. 7.12a). The results of the experiments are summarized in Fig. 7.12b. The solutions of NH_4NO_3 , KNO_3 , and CsNO_3 (1 M) desorbed only small amounts of ^{137}Cs from the WB. In addition, the desorption ratios of ^{137}Cs of these solutions remained almost unchanged with time. In contrast, ^{137}Cs was considerably desorbed by LiNO_3 and NaNO_3 , whereas $\text{Mg}(\text{NO}_3)_2$ and $\text{Ca}(\text{NO}_3)_2$ were not so effective at desorbing ^{137}Cs . The acidic solutions (HCl and HNO_3 , 0.1 M) also desorbed ^{137}Cs effectively from WB. In this experiment, the immersion time of WB in the ^{137}Cs solution to sorb radioactive Cs was 24 h. We extended this to 168 h, 336 h, and 672 h. Radioactive particles of WB collected from Fukushima, or WB which sorbed radioactive Cs in the field (“natural radioactive WB”), were also subjected to the same desorption experiment (Fig. 7.13). LiNO_3 and NaNO_3 solutions were effective in desorbing ^{137}Cs from WB when the sorption

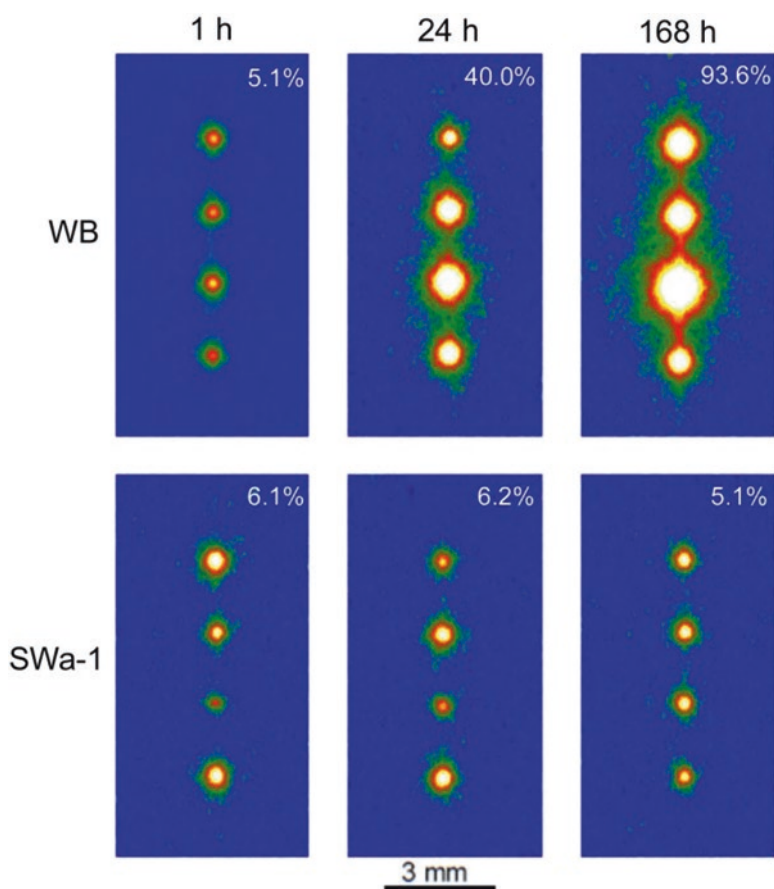


Fig. 7.11 A matrix of the readout images of IPs exposed by the substrates with four mineral particles of WB (top) and SWa-1 (bottom), reacted with 1.85 Bq ^{137}Cs solution for various immersion times which are shown at the top. Notice that only one mineral species was placed on the substrates and the mineral particles were different for each run. (Mukai et al. 2016a)

time was 24 h and 168 h. However, with a longer time, the desorption ratio was significantly decreased, becoming similar to NH_4NO_3 . In addition, radioactive Cs was hardly desorbed by these solutions from the natural radioactive WB. On the contrary, in the case of HCl, almost no decrease of the desorption ratios was observed with an extension in the sorption time. Furthermore, nearly half of the radioactivity of the natural radioactive WB was removed after treatment with HCl. In the treatment with the NH_4NO_3 solution, small amounts of the radioactive Cs were desorbed, irrespective of the sorption time. Probably these results in Fig. 7.13 indicate a kind of “aging effect”, namely as the sorption period is lengthened, Cs probably migrates along the interlayer regions of WB, to reside in more stable sites, and becomes almost impossible to remove by the normal ion-exchange process. Because natural radioactive WB particles collected from Fukushima have been in the field for more

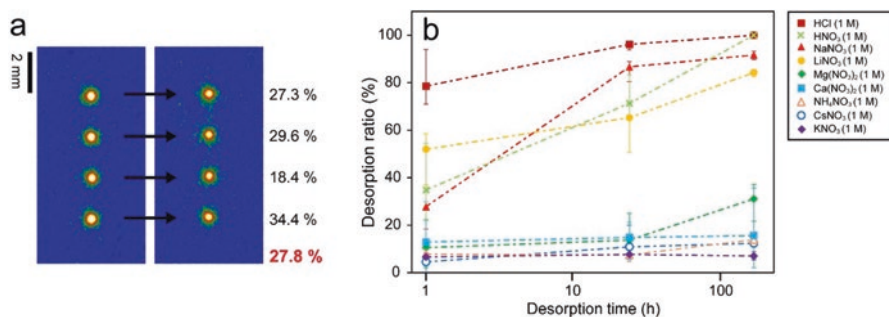


Fig. 7.12 (a) An example of the desorption experiments for the weathered biotite (WB). The readout IP images on the left and right were taken from WB particles before and after immersion, respectively, in an electrolyte solution (1 M NaNO₃ in this case) for a certain time. The figure represents the decrease ratio of the integrated IP intensity around the spots for each particle, and that at the bottom represents the average and is used as the “desorption ratio (%)” in (b). (b) Desorption ratios of ¹³⁷Cs from WB for various solutions and immersion times. For each sample, ¹³⁷Cs was sorbed to four particles of WB from a 50 μ l solution with 2.5 Bq for 24 h. WB particles sorbing ¹³⁷Cs were immersed in the electrolyte solutions 50 μ l. Error bars represent the minimum and maximum desorption ratios in four particles as shown in (a). (Mukai et al. 2018)

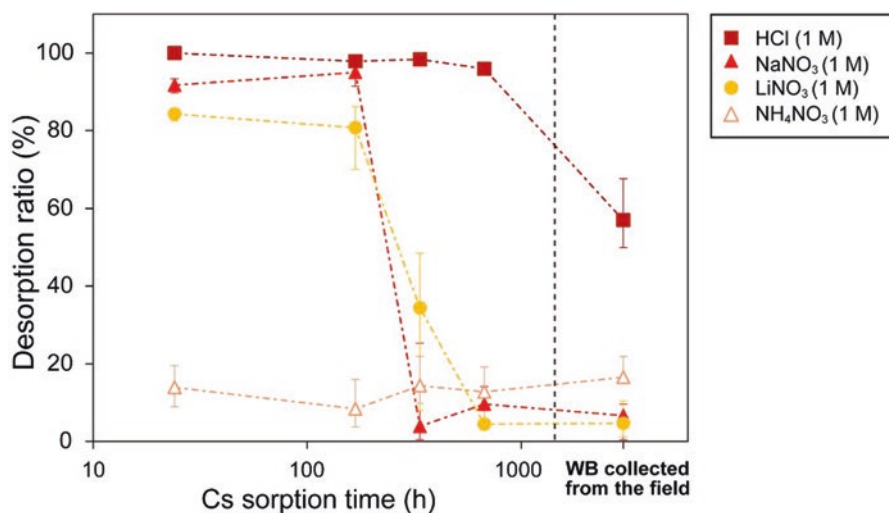


Fig. 7.13 Desorption ratios of WB as a function of ¹³⁷Cs-sorption time (24 h, 168 h, 336 h, and 672 h), and the desorption ratio of radioactive WB collected from the field at Fukushima. Desorption time was 168 h. (Mukai et al. 2018)

than 2 years, radiocesium has already been fixed at such stable sites. The effectiveness of HCl in removing a certain amount of Cs regardless of “aging” is probably due to the different leaching mechanism from ion-exchange; HCl partially dissolved the WB structure, particularly around the surface, and radiocesium fixed around the surface was leached to solutions with the other constituent elements.

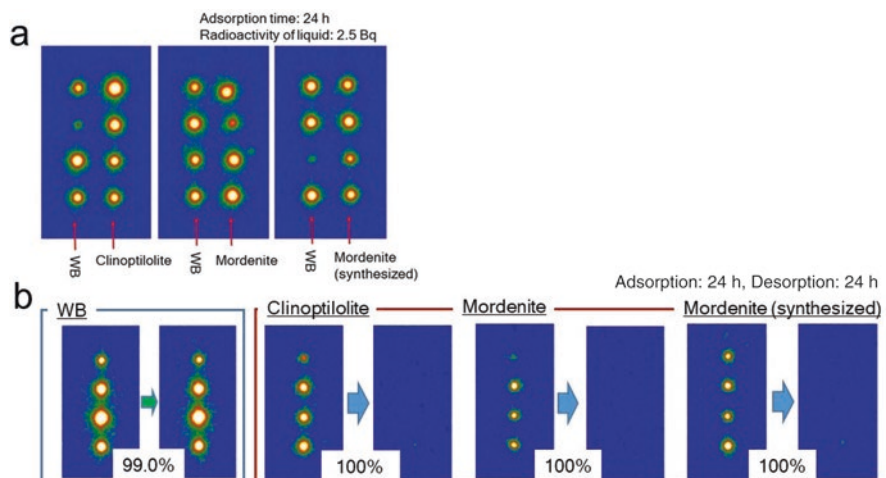


Fig. 7.14 (a) Comparison of the Cs-sorption abilities between WB and several zeolites. The experimental procedure was the same as those in Fig. 7.10. (b) Desorption properties of WB and several zeolites. The solution for desorption was CsCl (1 M)

These distinct properties of WB can explain several aspects of the radioactive contamination in Fukushima. For instance, most of the radiation that fell on the ground was trapped in a very shallow depth of the soil and has hardly moved into deeper soils (Honda et al. 2015). The distribution coefficients of radiocesium between sediments and river water are far larger (rich in sediment) in Fukushima than in Chernobyl (Konoplev et al. 2016). The transfer factors of radiation (radiocesium) from the soil to plants have decreased rapidly since the accident (e.g., Takeda et al. 2013). Probably these observations in the field in Fukushima are related to the high sorption and fixation ability of WB.

Cs in WB is hardly desorbed by ion-exchange with other alkali or alkali-earth cations in normal electrolyte solutions, particularly for WB that has remained for a long period in the field. Six years after the accident is probably long enough to change radiocesium in WB in such a passive state. Hence, decontamination of the radioactive soil by a process based on conventional ion-exchange is probably unlikely. Partial dissolution of WB in soils by strong acidic or basic solutions may be an answer but such solutions are not mild to the environment. Thermal decomposition of WB by calcination with additives is an alternative but the cost-performance ratio should be considered. On the other hand, WB is a promising candidate as an immobilizer of radiocesium, applicable to soil-improvement materials for agriculture or barriers at storage facilities for radioactive waste. For instance, Fig. 7.14 indicates the difference of sorption/desorption properties between WB and zeolites, typical sorbents used to remove radiocesium from contaminated water. The Cs-sorption ability from dilute Cs solutions is almost the same between WB and

zeolites, but the sorbed Cs in zeolites was easily desorbed by electrolyte solutions whereas that in WB was hardly removed, indicating that WB is superior as a retainer of radiocesium, if radiocesium should be immobilized permanently.

7.4 Conclusions

Radiocesium released from FDNPP has fallen on the ground where, fortunately or unfortunately, WB was abundant in the soil, and a large portion of radiocesium is now expected to be fixed in this mineral. In such areas, the dynamics of radiocesium should be considered on the basis of the character and properties of WB. Although our knowledge of WB has been increased considerably by the research carried out during the last few years, several substantial questions remain unanswered. For instance, the actual location(s) of dilute Cs in the WB structure, and the atomistic mechanism of “aging” as shown in Fig. 7.13, etc. are not clear yet. For future studies, these unknowns should be elucidated using fundamental research. Such research is still necessary because the radiation of ^{137}Cs will not rapidly decay for several decades and because similar disasters may occur in the future.

Acknowledgements The authors are grateful to Dr. S. Motai and Ms. E. Fujii for their collaboration in the research, Dr. T. Hatta and Dr. H. Yamada for donating the radioactively contaminated soils from Fukushima, Prof. Y. Watanabe for donating the zeolite specimens, Dr. A. Hirose, Prof. K. Tanoi, and Prof. TM. Nakanishi for the assistance with the sorption/desorption experiments using RI. This study was financially assisted by a Grant-in-Aid for Science Research (15H04222, 15H02149 and 24340133) by JSPS, Japan. This study was also supported through contracted research with the Japan Atomic Energy Agency (JAEA) for Fukushima environment recovery, entitled “Study on Cs adsorption and desorption process on clay minerals”.

References

- Adachi K, Kajino M, Zaizen Y, Igarashi Y (2013) Emission of spherical cesium-bearing particles from an early stage of the Fukushima nuclear accident. *Sci Rep* 3:2554
- Brouwer E, Baeyens B, Maes A, Cremers A (1983) Cesium and rubidium ion equilibria in illite clay. *J Phys Chem* 87:1213–1219
- Comans RNJ, Haller M, Depreter P (1991) Sorption of cesium on Illite – nonequilibrium behavior and reversibility. *Geochim Cosmochim Acta* 55:433–440
- Cornell RM (1993) Adsorption of cesium on minerals – a review. *J Radioanal Nucl Chem* 171:483–500
- Evans DW, Alberts JJ, Clark RA (1983) Reversible ion-exchange fixation of cesium-137 leading to mobilization from reservoir sediments. *Geochim Cosmochim Acta* 47:1041–1049
- Francis CW, Brinkley FS (1976) Preferential adsorption of Cs-137 to micaceous minerals in contaminated freshwater sediment. *Nature* 260:511–513

- Honda M, Matsuzaki H, Miyake Y, Maejima Y, Yamagata T, Nagai H (2015) Depth profile and mobility of ^{129}I and ^{137}Cs in soil originating from the Fukushima Dai-ichi Nuclear Power Plant accident. *J Environ Radioact* 146:35–43
- Japan Atomic Energy Agency (JAEA). Extension site of distribution map of radiation dose, etc. Available at: <http://ramap.jmc.or.jp/map/eng/>. Accessed 28 Dec 2015
- Japan Meteorological Agency. Archives of the past meteorological data (in Japanese). Available at: <http://www.data.jma.go.jp/obd/stats/etrn/index.php>. Accessed 28 Dec 2015
- Kikuchi R, Mukai H, Kuramata C, Kogure T (2015) Cs-sorption in weathered biotite from Fukushima granitic soil. *J Mineral Petrol Sci* 110:126–134
- Kogure T, Morimoto K, Tamura K, Sato H, Yamagishi A (2012) XRD and HRTEM evidences for fixation of cesium ions in vermiculite clay. *Chem Lett* 41:380–382
- Konoplev A, Golosov V, Laptev G, Nanba K, Onda Y, Takase T, Wakiyama Y, Yoshimura K (2016) Behavior of accidentally released radiocesium in soil-water environment: looking at Fukushima from a Chernobyl perspective. *J Environ Radioact* 151:568–578
- McKinley JP, Zachara JM, Heald SM, Dohnalkova A, Newville MG, Sutton SR (2004) Microscale distribution of cesium sorbed to biotite and muscovite. *Environ Sci Technol* 38:1017–1023
- Motai S, Mukai H, Watanuki T, Ohwada K, Fukuda T, Machida A, Kuramata C, Kikuchi R, Yaita T, Kogure T (2016) Mineralogical characterization of radioactive particles from Fukushima soil using μ -XRD with synchrotron radiation. *J Mineral Petrol Sci* 111:305–312
- Mukai H, Hatta T, Kitazawa H, Yamada H, Yaita T, Kogure T (2014) Speciation of radioactive soil particles in the Fukushima contaminated area by IP autoradiography and microanalyses. *Environ Sci Technol* 48:13053–13059
- Mukai H, Hirose A, Motai S, Kikuchi R, Tanoi K, Nakanishi TM, Yaita T, Kogure T (2016a) Cesium adsorption/desorption behavior of clay minerals considering actual contamination conditions in Fukushima. *Sci Rep* 6:21543
- Mukai H, Motai S, Yaita T, Kogure T (2016b) Identification of the actual cesium-adsorbing materials in the contaminated Fukushima soil. *Appl Clay Sci* 121–122:188–193
- Mukai H, Tamura K, Kikuchi R, Takahashi S, Yaita T, Kogure T (2018) Cesium desorption behavior of weathered biotite in Fukushima considering the actual radioactive contamination level of soils. *J Environ Radioact* 190–191:81–88
- Nakanishi TM (2016) An overview of our research. In: Nakanishi, Tanoi (eds) *Agricultural implications of the Fukushima nuclear accident. The first three years*. Springer Open, London
- Nakao A, Thiry Y, Funakawa S, Kosaki T (2008) Characterization of the frayed edge site of mica-ceous minerals in soil clays influenced by different pedogenetic conditions in Japan and northern Thailand. *Soil Sci Plant Nutr* 54:479–489
- National Institute of Material Science (NIMS). Database of promising adsorbents for decontamination of radioactive substances after Fukushima Daiichi Nuclear Power Plants accident. Available at: http://reads.nims.go.jp/index_en.html. Accessed 23 Nov 2017
- Ohnuki T, Kozai N (2013) Adsorption behavior of radioactive cesium by non-mica minerals. *J Nucl Sci Technol* 50:369–375
- Okumura T, Tamura K, Fujii E, Yamada H, Kogure T (2014) Direct observation of cesium at the interlayer region in phlogopite mica. *Microscopy* 63:65–72
- Poinssot C, Baeyens B, Bradbury MH (1999) Experimental and modelling studies of caesium sorption on illite. *Geochim Cosmochim Acta* 63:3217–3227
- Takeda A, Tsukada H, Nakao A, Takaku Y, Hisamatsu S (2013) Time-dependent changes of phytoavailability of Cs added to allophanic andosols in laboratory cultivations and extraction tests. *J Environ Radioact* 122:29–36

- Yamaguchi N, Mitome M, Akiyama-Hasegawa K, Asano M, Adachi K, Kogure T (2016) Internal structure of cesium-bearing radioactive microparticles released from Fukushima nuclear power plant. *Sci Rep* 6:20548
- Zachara JM, Smith SC, Liu CX, McKinley JP, Serne RJ, Gassman PL (2002) Sorption of Cs⁺ to micaceous subsurface sediments from the Hanford site, USA. *Geochim Cosmochim Acta* 66:193–211
- Zaunbrecher LK, Cygan RT, Elliott WC (2015) Molecular models of cesium and rubidium adsorption on weathered micaceous minerals. *J Phys Chem A* 119:5691–5700

Open Access This chapter is licensed under the terms of the Creative Commons Attribution 4.0 International License (<http://creativecommons.org/licenses/by/4.0/>), which permits use, sharing, adaptation, distribution and reproduction in any medium or format, as long as you give appropriate credit to the original author(s) and the source, provide a link to the Creative Commons license and indicate if changes were made.

The images or other third party material in this chapter are included in the chapter's Creative Commons license, unless indicated otherwise in a credit line to the material. If material is not included in the chapter's Creative Commons license and your intended use is not permitted by statutory regulation or exceeds the permitted use, you will need to obtain permission directly from the copyright holder.

